Fine-Grained Recognition in High-throughput Phenotyping
Supplemental Materials

Beichen Lyu Stuart D. Smith Keith A. Cherkauer
Purdue University, West Lafayette, IN
{lvb, smit1770, cherkaue}@purdue.edu

Abstract

This package of Supplemental Materials contains three items: 1) Datasets, 2) Invariance Proof of Radial Object Descriptor, and 3) Sample Filter Heatmaps.

1. Datasets

Datasets used in our experiments are anonymously shared at:

https://www.dropbox.com/s/p8rzqehytqred2h/datasets.zip?dl=0

This folder contains four High-throughput Phenotyping (HTP) datasets for Fine-Grained Recognition (FGR) applications which are respectively related to plant cultivars of soybean, arabidopsis, bean, and komatsuna. Each of the four datasets corresponds to notations used in our paper as: `HTP-Soy`, `Arabidopsis` [2], `Bean` [1], and `Komatsuna` [3]. For more details about `HTP-Soy`, please see our paper. For more details about the other three datasets, please see citations.

2. Invariance Proof of ROD

Below we prove that the newly proposed feature descriptor, Radial Object Descriptor (ROD), is invariant under scaling, rotation, and translation.

Theorem 1. *Radial Object Descriptor is invariant under uniform scaling, rotation, and translation.*

Proof. Based on Algorithm 1, this theorem can be formulated as

$$\frac{x_i - x_{\min}}{x_{\max} - x_{\min}} = \frac{x'_i - x'_{\min}}{x'_{\max} - x'_{\min}}, \forall i = 1, 2...|x|$$

where x and x' respectively denote the ROD before and after transformation.

Suppose that there is a transformation of translation by factor (t_1, t_2), rotation by angle θ, and uniform scaling by factor a. Then a contour pixel $e = \begin{bmatrix} e_1 \\ e_2 \end{bmatrix}$ will be transformed to $e' = \begin{bmatrix} e'_1 \\ e'_2 \end{bmatrix}$, which satisfies

$$\begin{bmatrix} e'_1 \\ e'_2 \\ 1 \end{bmatrix} = \begin{bmatrix} 1 & 0 & t_1 \\ 0 & 1 & t_2 \\ 0 & 0 & 1 \end{bmatrix} \begin{bmatrix} \cos\theta & -\sin\theta & 0 \\ \sin\theta & \cos\theta & 0 \\ 0 & 0 & 1 \end{bmatrix} \begin{bmatrix} a & 0 & 0 \\ 0 & a & 0 \\ 0 & 0 & 1 \end{bmatrix} \begin{bmatrix} e_1 \\ e_2 \\ 1 \end{bmatrix}$$
$$= \begin{bmatrix} \cos\theta \cdot a \cdot e_1 - \sin\theta \cdot a \cdot e_2 + t_1 \\ \sin\theta \cdot a \cdot e_1 + \cos\theta \cdot a \cdot e_2 + t_2 \\ 1 \end{bmatrix}$$

Similarly, a seed $s = \begin{bmatrix} s_1 \\ s_2 \end{bmatrix}$ will be transformed to $s' = \begin{bmatrix} s'_1 \\ s'_2 \end{bmatrix} = \begin{bmatrix} \cos\theta \cdot a \cdot s_1 - \sin\theta \cdot a \cdot s_2 + t_1 \\ \sin\theta \cdot a \cdot s_1 + \cos\theta \cdot a \cdot s_2 + t_2 \end{bmatrix}$. Then we can write $x'_i = ||e' - s'||_2$ as

$$\begin{aligned} x'_i &= \sqrt{(e'_1 - s'_1)^2 + (e'_2 - s'_2)^2} \\ &= \sqrt{\begin{matrix} (\cos\theta \cdot a \cdot (e_1 - s_1) - \sin\theta \cdot a \cdot (e_2 - s_2))^2 + \\ (\sin\theta \cdot a \cdot (e_1 - s_1) + \cos\theta \cdot a \cdot (e_2 - s_2))^2 \end{matrix}} \\ &= \sqrt{\begin{matrix} \cos^2\theta \cdot a^2 \cdot (e_1 - s_1)^2 + \sin^2\theta \cdot a^2 \cdot (e_2 - s_2)^2 + \\ \sin^2\theta \cdot a^2 \cdot (e_1 - s_1)^2 + \cos^2\theta \cdot a^2 \cdot (e_2 - s_2)^2 \end{matrix}} \\ &= a \cdot \sqrt{(e_1 - s_1)^2 + (e_2 - s_2)^2} \\ &= a \cdot x_i \end{aligned}$$

We can use similar procedures to show that $x'_{\max} = a \cdot x_{\max}$ and $x'_{\min} = a \cdot x_{\min}$. Now we can see that

$$\frac{x'_i - x'_{\min}}{x'_{\max} - x'_{\min}} = \frac{a \cdot (x_i - x_{\min})}{a \cdot (x_{\max} - x_{\min})} = \frac{x_i - x_{\min}}{x_{\max} - x_{\min}}$$

which concludes the proof.

□

3. Sample Filter Heatmaps

Using sample filter heatmaps, **figure 1** and **2** (see next two pages) illustrate the effectiveness of fusing ROD and Histogram of Oriented Gradients (HOG) in Softmax regression. Figure 1 is based on classifying 6 replicates (with different collection times) of arabidopsis plants into 2 classes while figure 2 is based on classifying 6 replicates (with different camera view angles) of soybean plots into 2 classes.

For the HOG feature, we present the visualizations of the most discriminative parts (top and bottom) based on the filter heatmaps of W_{HOG}. Observe that the most discriminative parts of arabidopsis plants and soybean plots are along their contours, which indicates the significance of features along contour.

For the ROD feature, we present the 1-dimensional RODs that are unfolded from 2-dimensional contours. Observe that even under the changes of collection time or camera's view angle, replicates in each class share RODs with very similar shapes. Also, we present the filter heatmaps of W_{ROD} in the form of 2-dimensional contours. Again, observe that most elements in RODs are very discriminative, which indicates the important cues provided by contour-based RODs, even though RODs' vector lengths are much smaller than HOGs'.

References

[1] Jeffrey A. Cruz, Xi Yin, Xiaoming Liu, Saif M. Imran, Daniel D. Morris, David M. Kramer, and Jin Chen. Multi-modality imagery database for plant phenotyping. *Machine Vision and Applications*, pages 735–749, 2016. 1

[2] Sarah Taghavi Namin, Mohammad Esmaeilzadeh, Mohammad Najafi, Tim B. Brown, and Justin O. Borevitz. Deep phenotyping: deep learning for temporal phenotype/genotype classification. *Plant Methods*, 14(1):66, 2018. 1

[3] Hideaki Uchiyama, Shunsuke Sakurai, Masashi Mishima, Daisaku Arita, Takashi Okayasu, Atsushi Shimada, and Rin ichiro Taniguchi. An easy-to-setup 3d phenotyping platform for komatsuna dataset. *IEEE International Conference on Computer Vision*, pages 2038–2045, 2017. 1

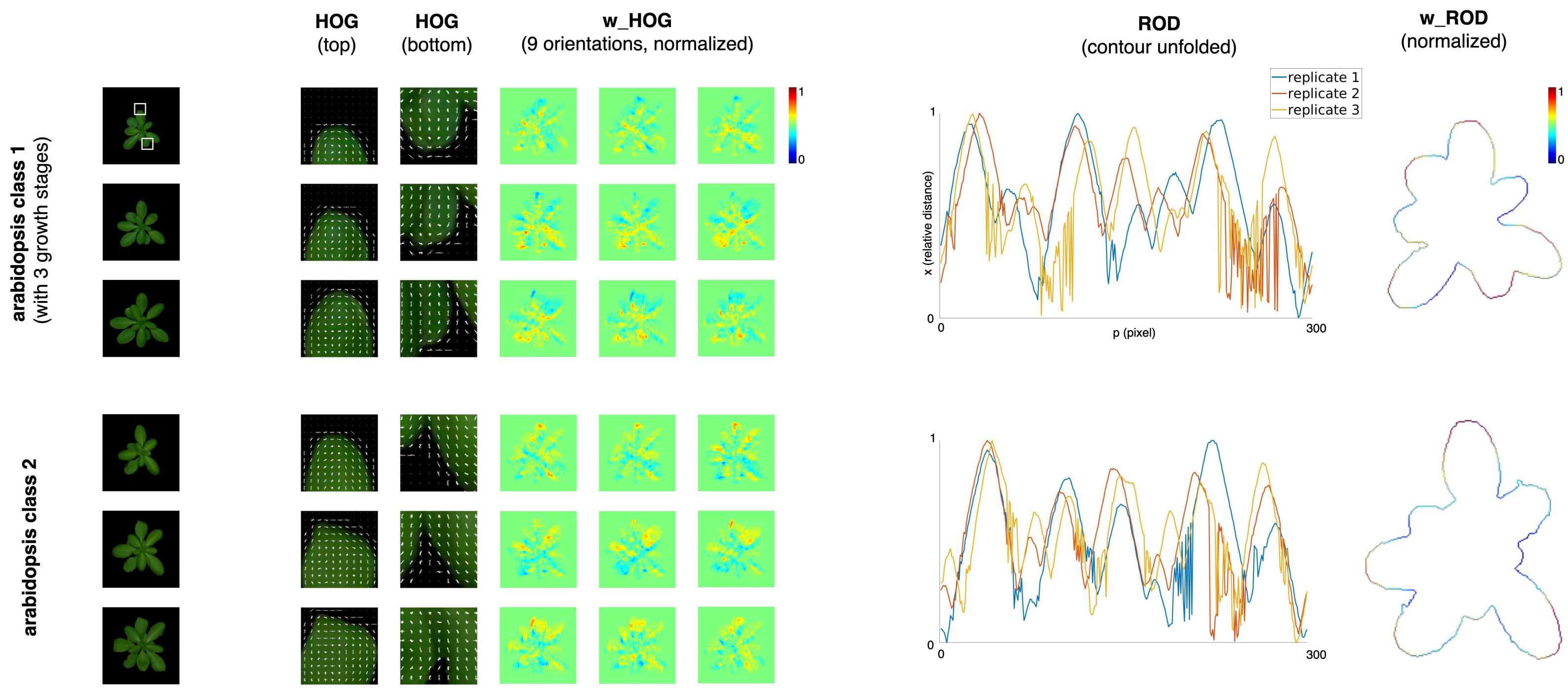

Figure 1: Sample features and filter heatmaps resulted from the fusion of HOG and ROD in Softmax regression for arabidopsis plants.

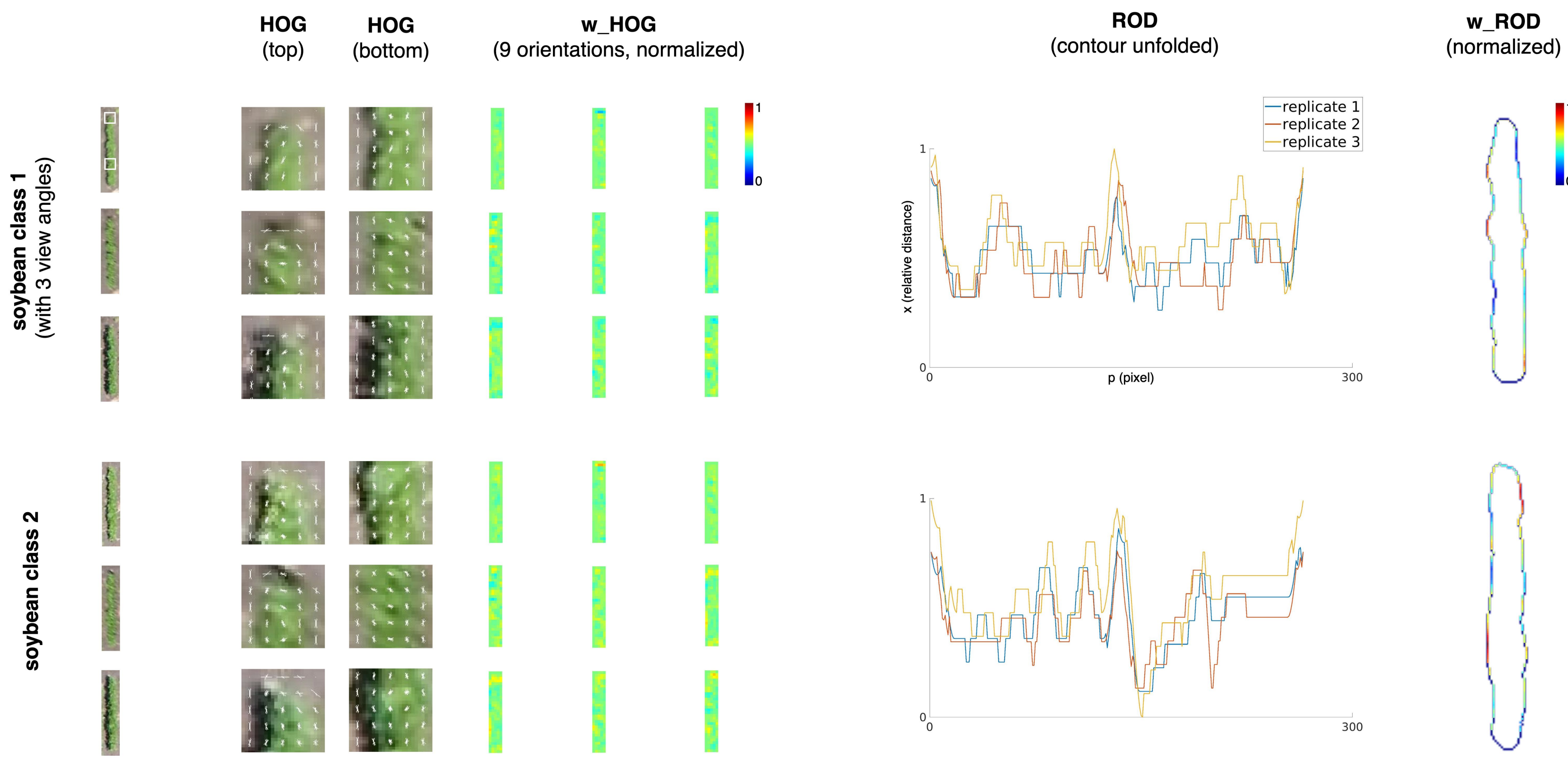

Figure 2: Sample features and filter heatmaps resulted from the fusion of HOG and ROD in Softmax regression for soybean plots.